On the Line Method apparent fracture toughness evaluations: experimental overview, validation and some consequences on fracture assessments

S. Cicero[1]*, T. García[1], V. Madrazo[2]

1) Dpto. Ciencia e Ingeniería del Terreno y de los Materiales, Universidad de Cantabria, Av/ Los Castros 44, 39005, Santander, Cantabria, Spain

2) Fundación Centro Tecnológico de Componentes (CTC), Parque Científico y Tecnológico de Cantabria (PCTCAN), C/ Isabel Torres nº 1, 39011, Santander, Spain

*corresponding author: ciceros@unican.es

Abstract

This paper analyses the capacity of the Line Method to provide evaluations of the apparent fracture toughness, which is the fracture resistance exhibited by materials in notched conditions. With this aim, the experimental results obtained in 555 fracture tests are homogeneously presented and compared to the Line Method evaluations. It is remarked that the Line Method provides adequate estimates of the apparent fracture toughness, and also that it conveniently addresses the physics of the notch effect. All this makes the Line Method a valuable scientific and engineering tool for the fracture assessment of materials containing notches.

Keywords: Line Method, Theory of Critical Distances, apparent fracture toughness, notch

1. Introduction

The load-bearing capacity of structural components is generally conditioned by the presence of stress risers such as cracks, notches, welded joints, corners. These stress risers take very different forms, and different approaches have been proposed to deal with the structural integrity of such components. This paper is focused on the notch-type defects (particularly, U-shaped notches), which may appear in structural components due to design details, mechanical damage, corrosion defects or fabrication defects.

When notches are blunt, it is overly conservative to proceed on the assumption that they behave like sharp cracks and to apply Fracture Mechanics criteria (i.e., such an

assumption may lead to unnecessary repairs or replacements, or to structural oversizing). In fact, as has been widely shown in the literature (e.g., [1-9]), components with non-sharp defects or notches exhibit an apparent fracture toughness that is greater than that obtained for cracked components. This generally has direct consequences on the load-bearing capacity of the structural components and also on their structural integrity assessments [4].

The literature (e.g., [7,8]) shows that there are two main failure criteria in the notch theory: the global criterion and the local criteria. The global criterion is analogous to the ordinary fracture mechanics approach, and establishes that fracture takes place when the notch stress intensity factor (K_ρ) reaches a critical value (K_ρ^c), where K_ρ defines the stress and strain fields in the vicinity of the notch tip, whereas K_I defines such fields in the crack tip. This approach is of unquestionable significance, but its application is very limited because of the lack of analytical solutions for K_ρ or/and standardized procedures for the experimental definition of K_ρ^c.

Meanwhile, local criteria are based on the stress-strain field at the notch tip. The most important ones are the Point Method (PM) and the Line Method (LM), both of them being methodologies of the Theory of Critical Distances (TCD) that can easily generate evaluations of the apparent fracture toughness exhibited by notched components. The resulting expression of the LM is particularly simple, and provides similar predictions to those generated by the PM [9]: therefore, for the sake of simplicity, the analysis here is focused on the LM estimations.

In any case, the evaluations provided by the LM (or the PM) have been validated for different materials (a sound review may be found in [9]), but such predictions have not been treated homogeneously and, therefore, they are not directly comparable. The

aim of this paper is to provide a homogenous analysis of a high number of apparent fracture toughness tests (555) performed on notched specimens under very different conditions (different materials, notch radii, testing specimens, testing temperatures, parameter calibration processes, etc.), providing a general validation of the LM. This allows general conclusions to be made concerning the use and the validity of the apparent fracture toughness evaluations obtained from the LM.

2. Theoretical background: the Line Method and apparent fracture toughness evaluations

The Theory of the Critical Distances (TCD) comprises a group of methodologies with a common aspect: they all use a characteristic material length parameter (the critical distance) when performing fracture assessments [9,10]. The origins of the TCD are located in the middle of the twentieth century [11,12], but in the last two decades this theory has had a wider development, providing answers to different scientific and engineering problems (e.g., [3,6, 13-20]).

The above-mentioned length parameter is generally referred as the critical distance, L, and in fracture analyses it follows the equation[9]:

$$L = \frac{1}{\pi}\left(\frac{K_{mat}}{\sigma_0}\right)^2 \qquad (1)$$

where K_{mat} is the material fracture toughness obtained for cracked specimens, and σ_0 is a characteristic material strength parameter, named the inherent strength. The last parameter (σ_0) is usually larger than the ultimate tensile strength (σ_u) and must be calibrated, although σ_0 coincides with σ_u in those situations where there is a linear-elastic behaviour at both the micro and the macro scales (e.g., fracture of ceramics and certain rocks).

There are different methodologies, within the TCD, allowing fracture analyses to be performed [9], such as the Point Method (PM), the Line Method (LM), the Imaginary Crack Method (ICM) and the Finite Fracture Mechanics (FFM). In any case, the evaluations made by these methodologies are very similar [9], and both the PM and the LM are particularly simple. Therefore, from now on, this theoretical overview is focused on these two methodologies.

The PM establishes that fracture occurs when the stress reaches the inherent strength, $\sigma_{0,}$ at a distance from the defect tip equal to L/2 [12,21,22]. Therefore, the failure criterion is:

$$\sigma\left(\frac{L}{2}\right)=\sigma_0 \tag{2}$$

The LM assumes that fracture occurs when the average stress along a certain distance, 2L, reaches the inherent strength, σ_0 [11, 22-24]. Therefore, the LM expression is:

$$\frac{1}{2L}\int_0^{2L}\sigma(r)dr=\sigma_0 \tag{3}$$

Moreover, both the PM and the LM provide expressions for the apparent fracture toughness (K^N_{mat}) exhibited by notched components. In the case of U-shaped notches (as those analysed in this paper) both the PM and LM may be applied considering the linear-elastic stress distribution at the notch tip provided by Creager and Paris [25], which is equal to that ahead of the crack tip but displaced a distance equal to $\rho/2$ along the x-axis, which is located in the notch midplane and has its origin at the crack tip [9,25] :

$$\sigma(r) = \frac{K_I}{\sqrt{\pi}} \frac{2(r+\rho)}{(2r+\rho)^{3/2}} \quad (4)$$

where K_I is the stress intensity factor for a crack with the same size as the notch, ρ is the notch radius and r is the distance from the notch tip to the point being assessed. Equation (4) was derived for long thin notches (i.e., notch depth >> notch radius) and is only valid for small distances from the notch tip (r << notch depth).

If the PM is applied, Equation (2) may be combined with Equation (4), giving [9]:

$$K_{mat}^{N} = K_{mat} \frac{\left(1+\frac{\rho}{L}\right)^{3/2}}{\left(1+\frac{2\rho}{L}\right)} \quad (5)$$

By considering the LM , Equation (3), together with Equation (4), we get [9]:

$$K_{mat}^{N} = K_{mat} \sqrt{1+\frac{\rho}{4L}} \quad (6)$$

This has implications from a practical point of view, given that it reduces the fracture analysis of a notched component to an equivalent situation of a cracked component, with the only particularity of considering K^{N}_{mat} instead of K_{mat}. Thus, fracture occurs when:

$$K_I = K_{mat}^{N} \quad (7)$$

Analogously, the authors have demonstrated [4,26] that notches may be analysed by using Failure Assessment Diagrams and substituting K_{mat} with K^{N}_{mat} in the definition of the K_r coordinate of the assessment point, which is defined as the ratio

between the applied stress intensity factor (K_I) and the material fracture resistance (K_{mat} for cracks and K^N_{mat} for notches) [27-29].

Both Equation (5) and Equation (6) have been validated in a number of papers (many of them are summarized in Ref. [9]), covering a wide range of materials.

However, the corresponding observations have been diverse or contradictory. In some cases a critical radius has been found below which the notch effect is negligible [39,40], whereas in other cases such a critical radius has not been detected[6,38]. On some occasions, the apparent fracture toughness remains approximately constant above a certain notch radius [6,9,39], and the experimental results differ from the LM or PM predictions (which predict a monotonically increasing fracture resistance when increasing the notch radius), whereas in other cases the experimental results continuously increase with the notch radius [9,38,40]. Some results of the apparent fracture toughness are conservative [2,9], whereas the predictions for other cases perfectly fit the experimental results or are non-conservative [3,6,9]. All this makes it necessary to undertake a sound analysis of the K^N_{mat} evaluations provided by the PM and the LM, providing a homogeneous treatment of the experimental data in order to find an answer to the above mentioned issues.

Finally, as discussed in Ref.[9], equations (5) and (6) provide similar K^N_{mat} evaluations. For this reason, the analysis shown below is focused on the LM predictions of K^N_{mat} (Equation (6)), although similar developments could easily be derived from the PM (Equation (5)).

3. Materials and methods

In the last few years, the present authors have published a number of papers showing the application of the LM to a wide range of materials: polymer PMMA [3],

aluminium alloy Al7075-T651 with two different orientations (LT and TL) [6], two common rocks (granite and oolitic limestone) [30], and four structural steels (S275JR, S355J2, S460M and S690Q) [2,31,32]. Moreover, such steels have been tested at 3 different temperatures of their corresponding Ductile-to-Brittle Transition Zone (DBTZ) and, in case of steels S275JR and S355J2, at temperatures equal to their Lower Shelf. Thus, the resulting experimental programme here collected comprises 20 different mechanical behaviours, which are summarized in Table 1. The total number of tests is 555, with fracture toughness values (cracked conditions) ranging from 0.72 $MPa \cdot m^{1/2}$ up to 157.4 $MPa \cdot m^{1/2}$, and L values varying from 0.0028 mm up to 6.04 mm. Some of the materials (e.g., PMMA, granite, limestone) presented a critical radius (larger than 4 mm for granite) below which the notch effect was negligible, whereas other materials (e.g., S275JR at five different temperatures) presented a clear notch effect (higher apparent fracture toughness) for the smallest analysed notch radius (0.15 mm). In the same way, some materials presented pure brittle behaviour (e.g., S275JR at -120 ºC, S355J2 at -196ºC, granite, limestone), whereas other materials presented limited ductile behaviour before the onset of cleavage fracture (e.g., the four steels at the different temperatures belonging to their corresponding DBTZ).

In all cases, the fracture toughness tests (in cracked specimens) and the apparent fracture toughness tests (in notched specimens) were performed following well-known standards [33,34] or procedures [35], whereas three different methodologies were employed for the calibration of the material critical distance (L). PMMA and Al7075-T651 were calibrated by using the Finite Element method and obtaining the stress fields at rupture in two specimens with different values of notch radius: applying the PM definition, both curves cross each other at a distance from the notch tip equal to L/2 [9]. The granite and the limestone were calibrated by the direct application of equation (1),

assuming that the inherent strength, $\sigma_{0,}$ is equal to the ultimate tensile strength, σ_u. Finally, the L value of the four steels at the different temperatures was calibrated by a least squares fitting of the experimental results.

Therefore, it is clear that the experimental results gathered here, and the corresponding application of the LM, represent an extensive range of situations. To perform a homogeneous analysis representing the 555 tests in a single graph (instead of 20 different graphs, one per mechanical behavior), the variables being represented need to be normalised. Usually, apparent fracture toughness results and LM evaluations are represented in a K^N_{mat} against $\rho^{1/2}$ plot. However, Equation (6) may be re-written in the following way:

$$\frac{K^N_{mat}}{K_{mat}} = \sqrt{1+\frac{1}{4}\left(\frac{\rho}{L}\right)} \qquad (8)$$

This immediately suggests a normalized representation of the experimental results in a (K^N_{mat}/K_{mat})against $(\rho/L)^{1/2}$ plot. That is, the apparent fracture toughness values are normalized by the fracture toughness obtained in cracked conditions, and the notch radii are normalized by the corresponding critical distance.

4. Results and discussion

Figure 1 shows the normalized representation of the 555 tests, together with the LM prediction provided by Equation (8), which has also been represented multiplied by 1.2 and 0.8 in order to visually capture the scatter of the results. Note that the scatter obtained in fracture tests is generally significant, especially in steels tested within the DBTZ. As an example, the experimental results obtained in steel S275JR at -90 ºC show that the apparent fracture toughness of specimens with 2.0 mm notch radius ($(\rho/L)^{1/2}$=18) varies between 3.61 and 13.23 times the corresponding fracture toughness

obtained in cracked conditions. That is, the same material tested with identical specimens under the same conditions presents a maximum value of apparent fracture toughness which is 13.23/3.61=3.66 times the minimum obtained value.

From the results shown in Figure 1, the following observations can be made:

(1) The LM captures the physics of the notch effect, given that the LM prediction adequately follows the tendency of the experimental results, which have been obtained for a wide variety of materials and conditions. This occurs not only for the materials for which the L value has been best fitted through least squares methodology, but also for the materials with the L value obtained by using FE modelling or by directly applying equation (1). Equation (8) may be expressed in a more general form as:

$$\frac{K_{mat}^{N}}{K_{mat}} = \sqrt{1+\frac{1}{M}\left(\frac{\rho}{L}\right)} \tag{9}$$

where M is a coefficient that may be experimentally fitted and whose theoretical value (when following the LM together with the Creager-Paris stress distribution) is 4. Now, if the least squares methodology is applied to the 555 experimental results in order to obtain the value of M that best fits Equation (9), the result is M = 4.02. This, of course, is influenced by the fact that many of the tests (those performed on the four steels being analysed) had been previously fitted through the least squares in order to calibrate L. However, even if only the tests performed in PMMA, Al7075-T651, granite and limestone are considered (161 tests, those which have not been calibrated by using the least squares methodology), the value of M providing the best fit is 5.07. This difference is not very significant in practice by taking into account that the term containing M is squared.

Figure 2 shows the difference between the LM prediction following equation (8) and the LM predictions when M is 5.07. It can be observed that the differences are not substantial, and also that, in both cases, the LM provides good evaluations of the experimental apparent fracture toughness results.

Note that the LM has provided good estimations even for those situations where the Creager-Paris equation has exceeded its theoretical limits. For example, the steels tested within the DBTZ presented a certain (limited) plasticity, whereas Creager-Paris equations is derived from linear-elastic conditions, and certain notches were not long (e.g., in the two rocks, the condition ´notch depth >> notch radius´ is not fulfilled for the larger values of radius).

(2) The notch effect is negligible as long as the ratio ρ/L is lower than one. That is, provided that the radius of the notch being analysed is lower than the material critical distance, the notch behaves as a crack. This may have significant consequences. For example, if $\rho<L$ the notch can be analysed by using ordinary fracture mechanics and employing K_{mat} (the fracture toughness obtained from cracked specimens) as the fracture resistance parameter. Futher, precracking processes may be avoided if it is ensured that the radius of the corresponding machined notch is lower than L (e.g., in granite, machined notches with a radius lower than 6.04 mm would be enough). Finally, the fact that no critical radius is observed on some occasions may be caused by the simple reason that the radius of the analysed notch is higher than L. As an example, in order to detect the critical radius in steel S460M at -140ºC, it would be necessary to machine notch radii below 0.0028 mm, something not feasible in practical terms.

(3) The LM provides good evaluations for high values of ρ/L. Such a ratio, also known as the Neuber number [36] was proposed by Madrazo et al. [6] as a tentative criterion to limit the validity of the LM (and PM) apparent fracture predictions, given that it was observed that this fracture parameter tended to remain constant in Al7075-T651 for ρ/L>100. This was also related to the shift from plane strain conditions to the plane stress onset when the notch radius increases, following the arguments provided by Taylor [9] to explain the experimental observations obtained by Irwin [37], Tsuji et al. [38], Wilshaw et al. [39], and Yokobori and Konosu [40]. The 555 results gathered here do not reveal any weakening of the notch effect, with a continuous increase of the apparent fracture toughness for ρ/L values as high as 714 (steel S460M at -140ºC), and 112 tests with ρ/L ratio values higher than 100.

(4) If the LM evaluations are to be used in structural integrity assessments, although Equation (8) captures the physics of the notch effect adequately, it may be unsafe on many occasions, given that it sometimes provides apparent fracture toughness values higher than those measured experimentally (as is shown in Figure 1, roughly one half of the results are located below the LM curve). In order to provide a fracture analysis tool to be used in structural integrity assessments, it is necessary to propose an expression that is capable of providing safe predictions of the apparent fracture toughness. With this purpose, an experimental M value equal to 20 is proposed here, the corresponding prediction curve being shown in Figure 2.

Moreover, in order to capture the scatter obtained in cracked conditions, a normal distribution has been considered for the K^N_{mat}/K_{mat} results at ρ/L=0 (cracked specimens). The standard deviation of the K^N_{mat}/K_{mat} results obtained

for cracked specimens is 0.1616, and then the K^N_{mat}/K_{mat} value associated to a 95% confidence level is 0.73 (when a normal distribution is assumed, the corresponding 95% level is equal to the mean, here 1.0, minus 1.645 times the standard deviation). The corresponding LM prediction is also shown in Figure 2, which arises from equation (10):

$$\frac{K^N_{mat}}{K_{mat}} = 0.73\sqrt{1+\frac{1}{20}\left(\frac{\rho}{L}\right)} \qquad (10)$$

6. Conclusions

The aim of this paper is to provide an extensive validation of the Line Method apparent fracture toughness evaluations through the homogeneous treatment of 555 fracture tests performed on notched specimens. The tests include 20 different mechanical behaviours, covering rocks, polymers and metals. The experimental values of the apparent fracture toughness (K^N_{mat}) have been normalized by the corresponding fracture toughness (K_{mat}) obtained in cracked conditions, whereas the notch radius (ρ) has been normalized by the corresponding critical distance (L). Thus, the 555 tests may be represented in a single (K^N_{mat}/K_{mat})-$(\rho/L)^{1/2}$ plot. The results demonstrate the capacity of the LM to capture the physics of the notch effect and to provide adequate estimations of the apparent fracture toughness. This adequacy is extensible to very high values of the ρ/L ratio (over 700). It has also been shown that the notch effect is negligible as long as the notch radius is lower than the material critical distance, something that may be important in the fracture characterization of materials with high values of L, which could avoid precracking processes. Finally, different experimentally-fitted expressions based on the LM have been proposed in order to provide conservative evaluations of the apparent fracture toughness to be used in structural integrity assessments.

Acknowledgement

The authors of this work would like to express their gratitude to the Spanish Ministry of Economy and Competitiveness for the financial support of the project MAT2010-15721: 'Análisis de integridad estructural en defectos tipo entalla', on the results of which this paper is based.

REFERENCES

[1] F. Berto, P. Lazzarin, Recent developments in brittle and quasi-brittle failure assessment of engineering materials by means of local approaches, Mat. Sci. Eng. R. 75 (2014) 1-48.

[2] S. Cicero, V. Madrazo, T. García, Analysis of notch effect in the apparent fracture toughness and the fracture micromechanisms of ferritic–pearlitic steels operating within their lower shelf, Eng. Fail. Anal. 36 (2014) 322–342.

[3] S. Cicero, V. Madrazo, I.A. Carrascal, Analysis of notch effect in PMMA by using the Theory of Critical Distances, Eng. Fract. Mech. 86 (2012) 56–72.

[4] S. Cicero, V. Madrazo, I.A. Carrascal, R. Cicero, Assessment of notched structural components using failure assessment diagrams and the theory of critical distances, Eng. Fract. Mech. 78 (2011) 2809–2825.

[5] F.J.Gómez, M. Elices, Fracture loads for ceramic samples with rounded notches, Eng. Fract. Mech. 73 (2006) 880-894.

[6] V. Madrazo, S. Cicero, I.A. Carrascal, On the point method and the line method notch effect predictions in Al7075-T651, Eng. Fract. Mech. 79 (2012) 363–379.

[7] L.S. Niu, C. Chehimi, G. Pluvinage, Stress field near a large blunted V notch and application of the concept of notch stress intensity factor to the fracture of very brittle materials, Eng. Fract. Mech. 49 (1994) 325–335.

[8] G. Pluvinage, Fatigue and fracture emanating from notch; the use of the notch stress intensity factor, Nucl. Eng. Des. 185 (1998) 173–184.

[9] D. Taylor, The theory of critical distances: a new perspective in fracture mechanics, Elsevier, UK, 2007.

[10] D. Taylor, M. Merlo, R. Pegley, M.P. Cavatorta, M.P., The effect of stress concentrations on the fracture strength of polymethylmethacrylate, Mater. Sci. Eng. A. 382 (2004) 288-294.

[11] H. Neuber, Theory of notch stresses: principles for exact calculation of strength with reference to structural form and material, Springer Verlag, Berlin, 1958.

[12] R.E. Peterson, Notch sensitivity, in: G. Sines, J.L. Waisman (Eds.), Metal fatigue., McGraw Hill, 1959, pp. 293-306.

[13] L. Susmel, D. Taylor, Fatigue design in the presence of stress concentrations, J. Strain Anal. Eng. Des. 38 (2003) 443-452.

[14] L. Susmel, D. Taylor, On the use of the Theory of Critical Distances to predict failures in ductile metallic materials containing different geometrical features, Eng. Fract. Mech. 75 (2008) 4410-4421.

[15] L. Susmel, D. Taylor, D., An elasto-plastic reformulation of the Theory of Critical Distances to estimate lifetime of notched components failing in the low/medium-cycle fatigue regime, J. Eng. Mater. Technol. 132 (2010) 021002132.

[16] D. Taylor, A mechanistic approach to critical-distance methods in notch fatigue, Fatig. Fract. Eng. Mater. Struct. 24 (2001) 215-224.

[17] D. Taylor, G. Wang, The validation of some methods of notch fatigue analysis, Fatig. Fract. Eng. Mater. Struct. 23 (2000) 387-394.

[18] D. Taylor, P. Bologna, K. Bel Knani, Prediction of fatigue failure location on a component using a critical distance method, Int. J. Fatig. 22 (2000) 735-742.

[19] A. Carpinteri, A. Spagnoli, S. Vantadori, D. Viappiani, A multiaxial criterion for notch high-cycle fatigue using a critical-point method, Eng. Fract. Mech. 75 (2008) 1864-1874.

[20] A. Carpinteri, C. Ronchei, A. Spagnoli, S. Vantadori, Lifetime estimation in the low/medium-cycle regime using the Carpinteri-Spagnoli multiaxial fatigue criterion, Theor. Appl. Fract. Mech. 73 (2014) 120-127.

[21] F.A. McClintock, Ductile fracture instability in shear, J. Appl. Mech. 25 (1958) 582-588.

[22] J.M. Whitney, R.J. Nuismer, Stress fracture criteria for laminated composites containing stress concentrations, J. Compos. Mater. 8 (1974) 253-265.

[23] V.V. Novozhilov, On a necessary and sufficient criterion for brittle strength, Prik. Mat. Mek. 33 (1969) 201-210.

[24] A. Seweryn, Brittle fracture criterion for structures with sharp notches, Eng. Fract. Mech. 47 (1994) 673-681.

[25] M. Creager, C. Paris, Elastic field equations for blunt cracks with reference to stress corrosion cracking, Int. J. Fract. 3 (1967) 247-252.

[26] V. Madrazo, S. Cicero, T. García, Assessment of notched structural steel components using failure assessment diagrams and the theory of critical distances, Eng. Fail. Anal. 36 (2014) 104-120.

[27] T.L. Anderson, Fracture mechanics: fundamentals and applications, third ed., CRC Press, Florida, 2005.

[28] BS 7910: 2013: Guide to methods for assessing the acceptability of flaws in metallic structures, 2013. British Standards Institution, London, 2013.

[29] FITNET Fitness-for-Service (FFS) Proceure - Volume 1, M. Kocak, S. Webster, J.J. Janosch, R.A. Ainsworth, R., Koers, (Eds.), GKSS Forschungzscentrum, Geesthacht, 2008.

[30] S. Cicero, T. García, J. Castro, V. Madrazo, D. Andrés, Analysis of notch effect on the fracture behaviour of granite and limestone: An approach from the Theory of Critical Distances, Eng. Geol. 177 (2014) 1-9.

[31] S. Cicero, V. Madrazo, T. García, Analysis of notch effect in the apparent fracture toughness and the fracture micromechanisms of ferritic–pearlitic steels operating within their lower shelf, Eng. Fail. Anal. 36 (2014) 322-342.

[32] S. Cicero, T. García, V. Madrazo, Application and validation of the Notch Master Curve in medium and high strength structural steels, J. Mech. Sci. Tech. (2015) Submitted.

[33] ASTM D5045-99, Standard Test Methods for Plane-Strain Fracture Toughness and Strain Energy Release Rate of Plastic Materials. American Society of Testing and Materials, Philadelphia, 1999.

[34] ASTM E1820-09e1, Standard test method for measurement of fracture toughness. American Society for Testing and Materials, Philadelphia, 2009.

[35] CEN/TS 14425-1:2003, Advanced technical ceramics-test methods for determination of fracture toughness of monolithic ceramics-part 1: guide to test method selection. European Committee for Normalization, 2003.

[36] D. Taylor, Applications of the theory of critical distances in failure analysis, Eng. Fail. Anal. 18 (2011) 543-549.

[37] G.R. Irwin, Structural aspects of brittle failure, App. Mat. Res. 3 (1964) 65-81.

[38] K. Tsuji, K. Iwase, K. Ando, An investigation into the location of crack initiation sites in alumina, polycarbonate and mild steel, Fatig. Fract. Eng. Mat. Struct. 22 (1999) 509-517.

[39] T.R. Wilshaw, C.A. Rau, A.S. Tetelman, A general model to predict the elastic-plastic stress distribution and fracture strength of notched bars in plane strain bending, Eng. Fract. Mech. 1 (1968) 191-211.

[40] T. Yokobori, S. Konosu, Effects of ferrite grain size, notch acuity and notch length on brittle fracture stress of notched specimens of low carbon steel, Eng. Fract. Mech. 9 (1977) 839-847.

NOMENCLATURE

K_{mat}	material fracture toughness
K^{N}_{mat}	apparent fracture toughness
K_I	stress intensity factor
K_ρ	notch stress intensity factor
K_ρ^c	critical notch stress intensity factor
L	material critical distance
M	fitting parameter in equation (9)
r	distance from the notch tip
ρ	notch radius
σ	applied stress
σ_u	ultimate tensile strength
σ_0	material strength parameter (the inherent strength)
DBTZ	Ductile-to-brittle Transition Zone
FE	Finite Elements method
LM	Line Method
LS	Lower Shelf
PM	Point Method

TCD	Theory of Critical Distances
US	Upper Shelf

Tables

Table 1. Summary of the experimental results analysed in this paper (LS: Lower Shelf; DBTZ: Ductile-to-Brittle Transition Zone; FE: Finite Element method).

Material	Number of tests	Notch radii (mm)	K_{mat} (MPa·m$^{1/2}$)	L (mm)	Calibration method (L)
PMMA	32	0-2.5	2.04	0.1050	FE
Al7075-T651 LT	23	0-2.0	27.01	0.0150	FE
Al7075-T651 TL	24	0-2.0	26.65	0.0215	FE
Granite	41	0-10	1.24	6.04	Eq. (1)
Limestone	41	0-10	0.72	2.71	Eq. (1)
S275JR (-120ºC, LS)	23	0-2.0	48.80	0.0137	Best fit
S275JR (-90ºC, LS)	24	0-2.0	62.72	0.0062	Best fit
S275JR (-50ºC, DBTZ)	24	0-2.0	80.60	0.0049	Best fit
S275JR (-30ºC, DBTZ)	24	0-2.0	100.7	0.0061	Best fit
S275JR (-10ºC, DBTZ)	34	0-2.0	122.8	0.0083	Best fit
S355J2 (-196ºC, LS)	24	0-2.0	31.27	0.0198	Best fit
S355J2 (-150ºC, DBTZ)	21	0-2.0	60.56	0.0084	Best fit
S355J2 (-120ºC, DBTZ)	22	0-2.0	146.6	0.0168	Best fit
S355J2 (-100ºC, DBTZ)	35	0-2.0	157.4	0.0140	Best fit
S460M (-140ºC, DBTZ)	24	0-2.0	45.60	0.0028	Best fit
S460M (-120ºC, DBTZ)	24	0-2.0	88.29	0.0075	Best fit
S460M (-100ºC, DBTZ)	33	0-2.0	88.58	0.0053	Best fit
S690Q (-140ºC, DBTZ)	24	0-2.0	69.11	0.0069	Best fit
S690Q (-120ºC, DBTZ)	24	0-2.0	103.8	0.0131	Best fit
S690Q (-100ºC, DBTZ)	34	0-2.0	125.4	0.0170	Best fit

Figures

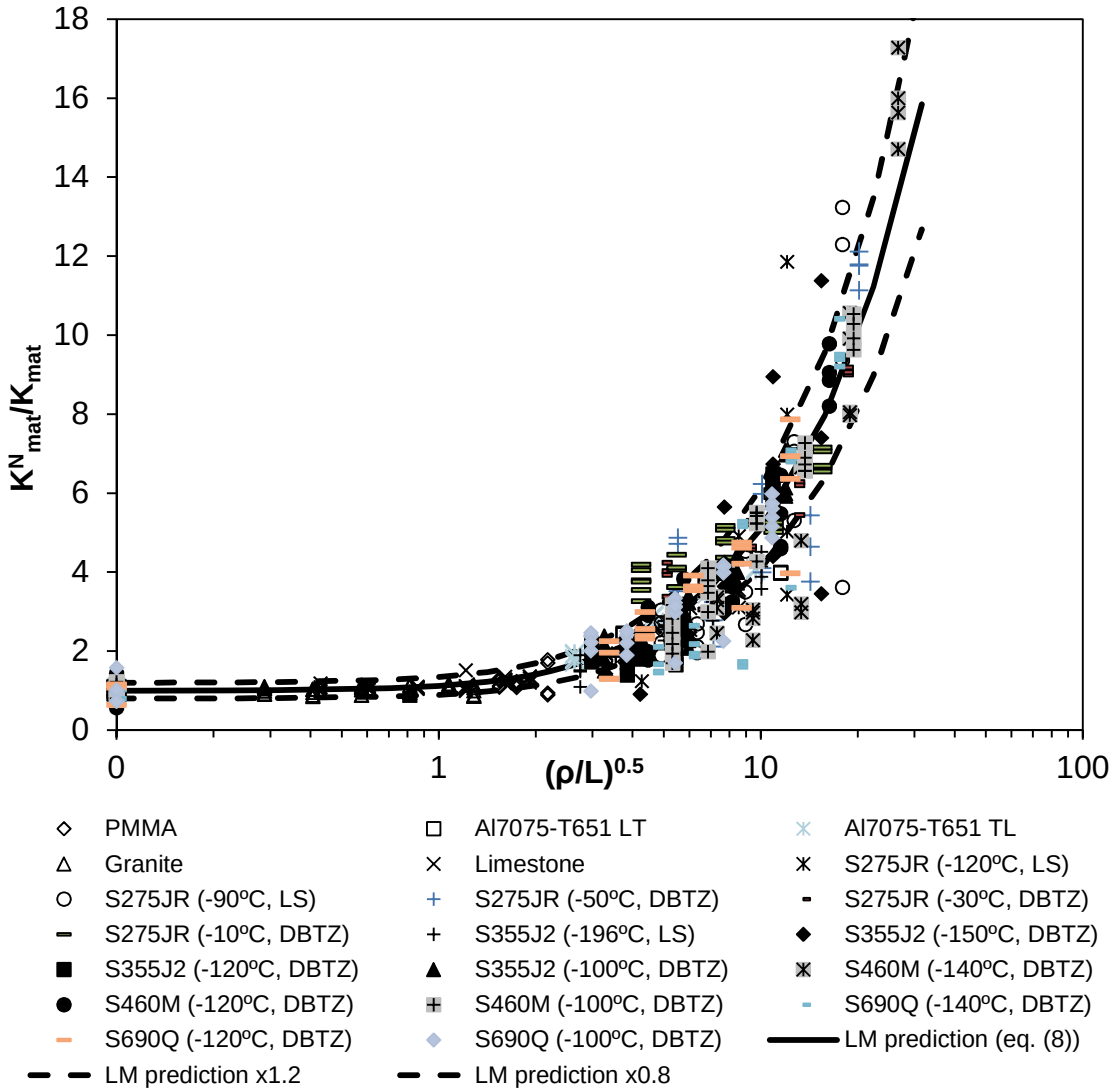

Figure 1. Normalised representation of the 555 fracture tests and comparison to the LM predictions.

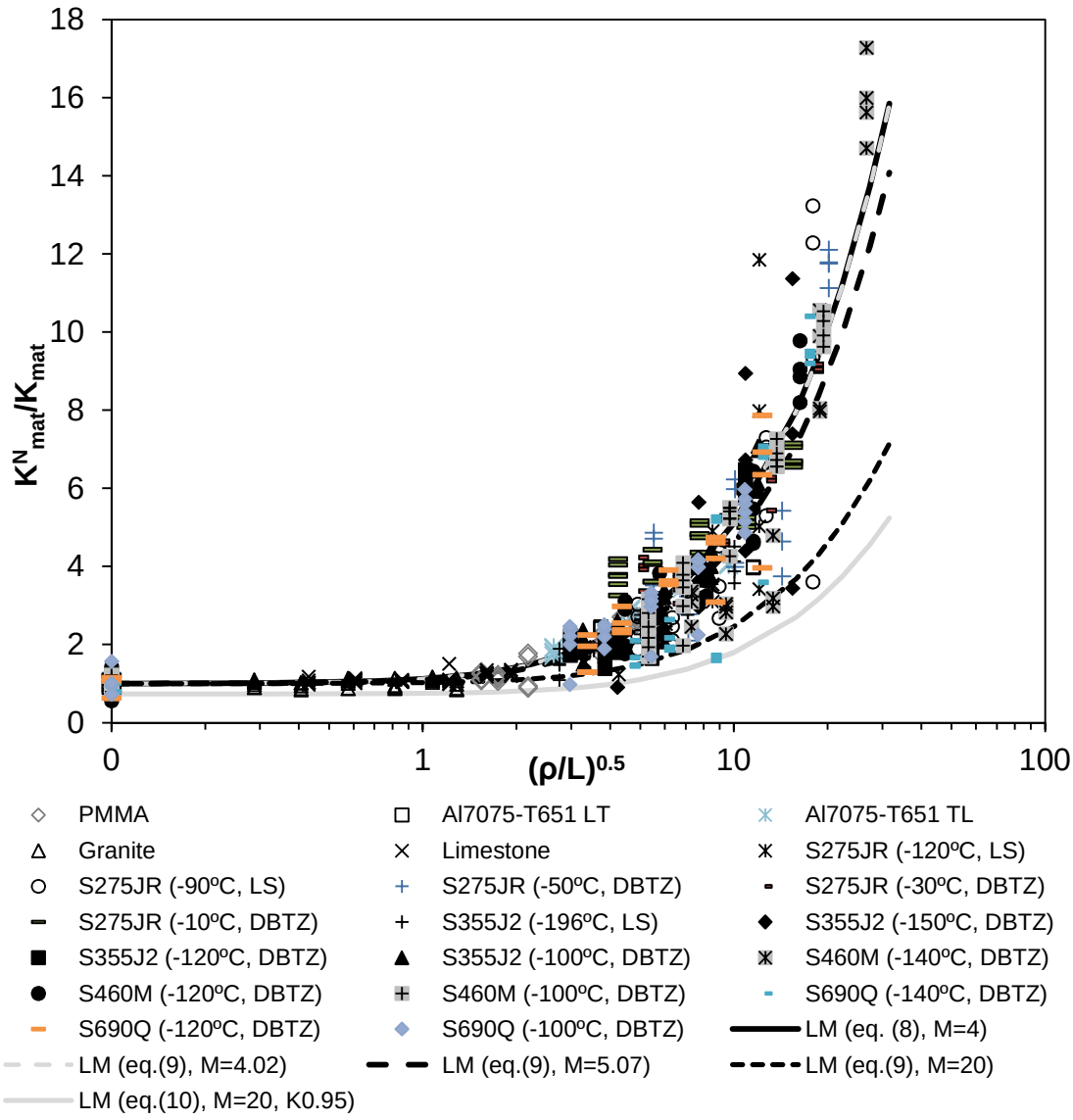

Figure 2. Normalised representation of the 555 fracture tests and comparison to the LM predictions when using equation (8), equation (9) (M=4.02, M=5.07 and M=20) and equation (10).